Dalton Transactions

PAPER

View Article Online
View Journal | View Issue

Cite this: *Dalton Trans.*, 2014, **43**, 8048

A new fluorescent probe for Zn^{2+} with red emission and its application in bioimaging†

Yiqun Tan, Min Liu, Junkuo Gao, Jiancan Yu, Yuanjing Cui, Yu Yang* and Guodong Qian*

Received 16th January 2014,
Accepted 10th March 2014

DOI: 10.1039/c4dt00167b

www.rsc.org/dalton

A new fluorescent probe, (*E*)-3-(3-(4-([2,2′:6′,2″-terpyridin]-4′-yl)phenyl)acryloyl)-7-(diethylamino)-2*H*-chromen-2-one (ZC-F4), composed of coumarin as the fluorophore and terpyridine as the receptor was designed and synthesized. This probe showed good selectivity and sensitivity towards Zn^{2+} even at the ppb level with significant variation of emission wavelength (more than 100 nm shifts) after combination with Zn^{2+}. One can observe that the emission colour changed from green to red. A Job's plot test suggested a 1 : 1 stoichiometry between ZC-F4 and Zn^{2+}, and the theoretical calculation based on density functional theory has been carried out to gain an insight into the sensing mechanism. Furthermore, imaging of Zn^{2+} in cells was also performed to test its feasibility in biology. This fluorescence probe should be a promising candidate for applications in cell-imaging, environment protection, water treatment and safety inspection.

Introduction

As the second most abundant transition metal ion in the human body, zinc plays an important role in gene transcription, regulation of metalloenzymes, neural signal transmission and apoptosis.[1–5] Its deficiency causes acrodermatitis enteropathica,[6] while excess zinc may also cause serious neurological disorders such as Alzheimer's and Parkinson's diseases.[7–9] It is found that the imbalance in zinc may cause several health problems including superficial skin diseases, prostate cancer, diabetes, and brain diseases.[10–12] Thus, extensive research effort has been devoted to the quantitative measurement of trace Zn^{2+} *in vivo*.[13–15] Because of the lack of spectroscopic signature of Zn^{2+}, a fluorescence probe has become one of the best options for detecting and tracking Zn^{2+} in cell-imaging and neurobiological experiments.[16]

In recent years, a number of fluorescent probes for detecting Zn^{2+} have been developed and most of them exhibit good performance in cellular use.[17–27] However, many fluorescence sensors still have problems of selectivity, especially interference from Cd^{2+} which possesses very similar chemical properties to Zn^{2+} because of their location in the same group. Recently, Jiang *et al.* have reported an inspired distinguishing method for Zn^{2+} and Cd^{2+} by introducing the carbonyl group.[28,29] Ng *et al.* designed two fluorescence sensors for differential detection of Zn^{2+} and Cd^{2+} based on BODIPY which can respond towards Zn^{2+} and Cd^{2+} respectively.[30] Lin *et al.* developed a single probe that displayed a distinct response to Zn^{2+} and Cd^{2+} depending on different anions.[31] Nevertheless, there have not been any reports about the application of these probes in cell-imaging.

The development of a novel fluorescence probe for metal ions with a high sensitivity and selectivity has long concerned our group.[32–35] We have developed a new fluorescence probe ZC-F1 based on the intra-molecular transfer (ICT) effect for recognizing Zn^{2+} from Cd^{2+} with the detection limit at the ppb level.[32] But it cannot be used in bio-imaging for the following reasons: (a) the poor solubility of ZC-F1 in aqueous solution restricts its application *in vivo*. (b) The quantum yield of fluorophores bearing the ICT effect usually reduces too much for practical application after the electron withdrawing group combines with metal ions, especially in solvents with high polarity, for the decrease of the energy gap between the ground state and the excited state.[36–39] (c) ZC-F1 emits green fluorescence after combining with Zn^{2+} with the emission located around 500 nm, while a longer wavelength is needed for bio-imaging. To overcome these obstacles, a new fluorescence probe highly sensitive and selective towards Zn^{2+} with better solubility and higher quantum yield is required.

Herein, we report a new fluorescence probe, (*E*)-3-(3-(4-([2,2′:6′,2″-terpyridin]-4′-yl)phenyl)acryloyl)-7-(diethylamino)-2*H*-chromen-2-one (ZC-F4). This probe contains 7-diethylaminocoumarin, which is known to be a water soluble fluorophore, and terpyridine as the receptor for Zn^{2+}.[40] To alleviate

State Key Laboratory of Silicon Materials, Cyrus Tang Center for Sensor Materials and Applications, Department of Materials Science & Engineering, Zhejiang University, Hangzhou, China. E-mail: gdqian@zju.edu.cn, yuyang@zju.edu.cn

† Electronic supplementary information (ESI) available: Supplementary spectra data. See DOI: 10.1039/c4dt00167b

the fluorescence decrease induced by metal ion binding, the carbonyl group is introduced as the electron withdrawing group, which conjugates with both coumarin and terpyridine. Then, Zn^{2+} will influence the electronegativity of terpyridine instead of carbonyl directly. Thus, the influence of metal ions on the energy gap will be reduced largely and a fluorescence enhancement in aqueous solution can be expected, making it possible to detect and track Zn^{2+} in cell-imaging and cancer-biological experiments.

Experimental section

Reagents and apparatus

Solvents and reagents were obtained from commercial sources and used as received without further purification.

^{1}H NMR spectra were recorded in $CDCl_3$ or DMSO-D6 on a 500 MHz Bruker Avance DMX500 spectrometer with tetramethysilane (TMS) as an internal standard. Elemental analysis was performed using a Thermo Finnigan Flash EA1112 microelemental analyzer. Differential scanning calorimetry (DSC) was performed on a Netzsch Instruments 200 F3 at a heating rate of 10 K min^{-1} under a nitrogen atmosphere. Inductively coupled plasma spectroscopy (ICP) was performed on a Thermo XSENIES ICP-MS. Fluorescence emission spectra and excitation spectra were obtained on a Hitachi F4600 fluorescence spectrophotometer. UV-vis absorption spectra were obtained using a Perkin-Elmer Lambda spectrophotometer. All the theoretical calculations were performed based on density functional theory (DFT) at the B3LYP/6-31G(d) level.[41,42] The solvent effect on molecular geometries was included by means of the polarizable continuum model (PCM).[43,44] Based on the optimized geometry, all the molecular orbitals were calculated at the same level. All the calculations were performed in Gaussian09 software.[45] Fluorescence quantum yield was measured with the integrating sphere on an Edinburgh Instrument F900. Fluorescence images were obtained on confocal laser scanning microscopes (CLSM, fluoview FV1000, Olympus).

Synthesis

3-Acetyl-7-(diethylamino)-2*H*-chromen-2-one (1). Ethyl-acetoacetate (1.95 g, 15 mmol) and 4-diethylamino-salicylaldehyde (1.93 g, 10 mmol) were added into the solution of EtOH (20 mL), followed by the addition of piperidine (0.2 mL). The resulting mixture was refluxed for 6 h and then cooled to room temperature. The yellow crystal was filtered and recrystallization was performed in EtOH to get a pure product (1.55 g, 60%). ^{1}H NMR (500 MHz, $CDCl_3$): δ = 1.24 (t, 6H, J = 7 Hz, CH_2CH_3), 2.68 (s, 3H, $COCH_3$), 3.45 (m, 4H, J = 7 Hz, CH_2CH_3), 6.47 (d, 1H, J = 2.5 Hz, ArH), 6.62 (d, 1H, J = 9 Hz, ArH), 7.39 (d, 1H, J = 4 Hz, ArH), 8.44 (s, 1H, ArH). Anal. calcd for $C_{15}H_{17}NO_3$: C, 69.48; N, 5.40; H, 6.61. Found: C, 69.83; N, 5.44; H, 6.64.

4′-(*p*-Methylphenyl)-2,2′:6′,2″-terpyridine (2). To a solution of 4-methylbenzaldehyde (0.65 g, 5.4 mmol) and 2-acetylpyridine (1.3 g, 10.8 mmol) in methanol (120 mL) was added NaOH (0.22 g, 5.4 mmol) and NH_4OH (30 mL). The mixture was refluxed for 12 h, and then cooled down to room temperature. The precipitate was filtered and washed with methanol and water to obtain a white powder (1.05 g, 40%). ^{1}H NMR (500 MHz, $CDCl_3$): δ = 2.34 (s, 3H, CH_3), 7.44 (s, 2H, ArH), 7.67 (d, 2H, J = 2 Hz, ArH), 7.85 (d, 2H, J = 8 Hz, ArH), 7.97 (s, 2H, ArH), 8.74 (d, 2H, J = 7 Hz, ArH), 8.78 (t, 4H, J = 12 Hz, ArH). Anal. calcd for $C_{22}H_{17}N_3$: C, 81.71; N, 12.99; H, 5.30. Found: C, 81.59; N, 13.10; H, 5.31.

4-([2,2′:6′,2″-Terpyridin]-4′-yl)benzaldehyde (3). 1 (1.0 g, 3.1 mmol) was added into the solution of CCl_4 (20 mL) and stirred for 15 min under an atmosphere of Ar_2. Then, benzoyl peroxide (0.049 g, 0.2 mmol) and *N*-bromosuccinamide (1.23 g, 6.2 mmol) were added into the solution followed by reflux for 24 h. The solution was cooled to room temperature and evaporated. The resulting yellow solid was then added into the solution of $CaCO_3$ (1.0 g, 10 mmol), 1,4-dioxane (40 mL) and water (10 mL) and refluxed for another 24 h. The mixture was then cooled to room temperature, evaporated and purified by chromatography, using EtOAC and petroleum (1 : 2) as eluents, affording a pale solid **3** (0.50 g, 48%). ^{1}H NMR (500 MHz, $CDCl_3$): δ = 7.35 (m, 2H, J = 5 Hz, ArH), 7.87 (m, 2H, ArH), 8.01 (m, 4H, J = 8 Hz, ArH), 8.66 (d, 2H, J = 8 Hz, ArH), 8.72 (t, 4H, ArH), 10.8 (s, 1H, CHO). Anal. calcd for $C_{22}H_{15}N_3O$: C, 78.32; N, 12.46; H, 4.48. Found: C, 78.39; N, 12.50; H, 4.41.

(*E*)-3-(3-(4-([2,2′:6′,2″-Terpyridin]-4′-yl)phenyl)acryloyl)-7-(diethylamino)-2*H*-chromen-2-one (ZC-F4). 1 (1.55 g, 6 mmol) and **3** (1.34 g, 4 mmol) were resolved in $CHCl_3$ (20 mL) followed by the addition of piperidine (0.1 mL) and acetate acid (0.2 mL) and refluxed for 24 h. After cooling to room temperature, the resulting mixture was then extracted three times. The organic phase was combined, and dried with $MgSO_4$. The solvent was removed under reduced pressure and the remaining black powder was purified by chromatography using CH_2Cl_2 and EtOAC (20 : 1) to yield an orange solid **ZC-F4** (1.41 g, 61%). ^{1}H NMR (500 MHz, $CDCl_3$): δ = 1.25 (t, 6H, J = 5 Hz, CH_2CH_3), 3.47 (m, 4H, J = 7.5 Hz, CH_2CH_3), 6.50 (s, 1H, ArH), 6.63 (d, 1H, J = 9 Hz, ArH), 7.36 (m, 2H, ArH), 7.43 (d, 1H, J = 9 Hz, ArH), 7.82 (d, 2H, J = 8 Hz, CH=CH), 7.88 (m, 3H, ArH), 7.94 (d, 2H, J = 8 Hz, ArH), 8.23 (d, 1H, J = 16 Hz, ArH), 8.57 (s, 1H, ArH), 8.67 (d, 2H, J = 8 Hz, ArH), 8.74 (m, 4H, ArH). Anal. calcd for $C_{37}H_{30}N_4O_3$: C, 76.80; N, 9.68; H, 5.23. Found: C, 76.69; N, 9.80; H, 5.31.

Zn(ZC-F4)$(NO_3)_2(H_2O)_2$ (ZC-F4–Zn). ZC-F4 (0.058 g, 0.1 mmol) was resolved in $CHCl_3$ (3 mL) followed by the addition of $Zn(NO_3)_2$ (0.057 g, 0.3 mmol) in 5 mL methanol. Upon mixing, a deep red suspension formed immediately. The resulting mixture was stirred for another 15 min to ensure reaction completion. The red solid was obtained by filtration and then washed with ethanol (5 mL × 3). ^{1}H NMR (500 MHz, DMSO-D6): δ = 1.17 (t, 6H, J = 7 Hz, CH_2CH_3), 3.53 (m, 4H, CH_2CH_3), 6.64 (s, 1H, ArH), 6.85 (d, 1H, J = 8.5 Hz, ArH), 7.52 (t, 1H, J = 6 Hz, ArH), 7.74 (d, 1H, J = 9 Hz, ArH), 7.85 (m, 1H, ArH), 7.99 (m, 2H, ArH), 8.04 (d, 1H, J = 8 Hz, ArH), 8.12 (d, 2H, J = 8 Hz, CH=CH), 8.31 (t, 2H, J = 7.5 Hz, ArH), 8.54 (d, 2H, J = 8 Hz, ArH), 8.67 (s, 1H, ArH), 8.91 (d, 1H, J = 4 Hz), 9.10 (d, 1H, J = 8 Hz, ArH), 9.18 (d, 2H, J = 8.5 Hz, ArH), 9.46 (s, 1H,

ArH). Anal. calcd for $C_{37}H_{34}N_6O_{11}Zn$: C, 55.27; N, 10.45; H, 4.26. Found: C, 55.00; N, 10.37; H, 4.04.

To certify the ratio between ZC-F4 and Zn^{2+} in ZC-F4–Zn, an ICP experiment was conducted by resolving 5 mg complex into 20 mL aqueous solution (DMSO–H_2O = 1 : 99) followed by the addition of 100 μL hydrochloric acid. The concentration of Zn^{2+} found in the solution is 20.5 mg L^{-1}, which agrees with that calculated (20.3 mg L^{-1}).

Cell culture

HeLa human cervical carcinoma cells were cultured in Dulbecco's Modified Eagle's Medium (DMEM, Neuronbc) supplemented with 10% fetal bovine serum (FBS, Sijiqing), penicillin (100 units ml^{-1}, Boster), and streptomycin (100 μg mL^{-1}, Boster). Two days before imaging, the cells were plated on glass-bottom dishes. For labeling, the growth medium was removed and replaced with DMEM without FBS. The cells were treated and incubated with 10 μL of 1 mM ZC-F4 in DMSO stock solution (10 μM ZC-F4) at 37 °C under 5% CO_2 for 15 min, and were provided with 5 μL of fresh medium that contained either 1 mM or 0 mM $ZnCl_2$. Then, the cells were incubated for another 15 min under the conditions mentioned above. Prior to imaging, cells were rinsed three times with phosphate buffered saline (PBS).

Results and discussion

Design and synthesis of ZC-F4

In the newly designed fluorescence probe ZC-F4, 7-diethylaminocoumarin is selected as the fluorophore to improve its solubility in water, and 2,2′,6′,2″-terpyridine is selected as the receptor for Zn^{2+} owing to its good performance in previous work. In addition, the amino group possesses a strong electron-donating ability, which may strengthen the ICT effect, and large Stokes' shifts, leading to red emission.[46–49] However, unlike ZC-F1, the fluorophore and the receptor are not conjugated directly, but linked *via* the carbonyl group. So ICT is established between the carbonyl group and the diethylamino part,[50–52] while terpyridine impacts on the carbonyl group with its weak electron-withdrawing ability. As a result, the zinc ions will indirectly influence the electronegativity of the electron acceptor after combining with terpyridine, which suggests a weak influence on the ICT energy level. Thus, an improved fluorescence emission of ZC-F4 in aqueous solution can be expected.

As shown in Scheme 1, the compound ZC-F4 can be synthesized in several steps from commercially available chemicals in high yield. Details of the synthesis are described in the Experimental section.

Optical response of probe ZC-F4

To test its feasibility for Zn^{2+} detection, the fluorescence spectra and the response of ZC-F4 after titrating with Zn^{2+} were first studied in aqueous solution (water–DMSO = 99 : 1). As shown in Fig. 1(a), a broadband emission spectrum with

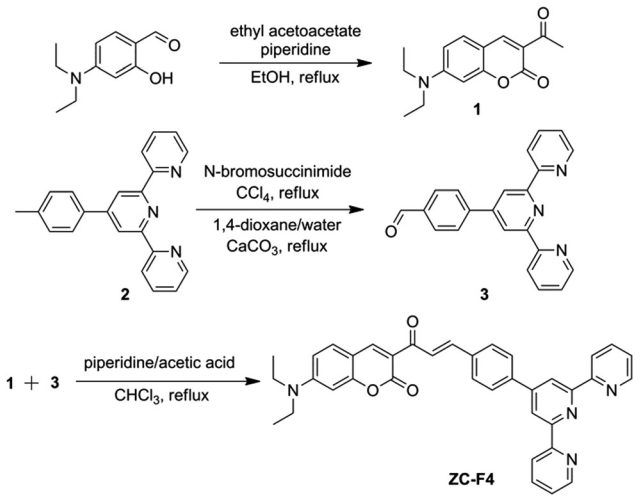

Scheme 1 Synthesis of ZC-F4.

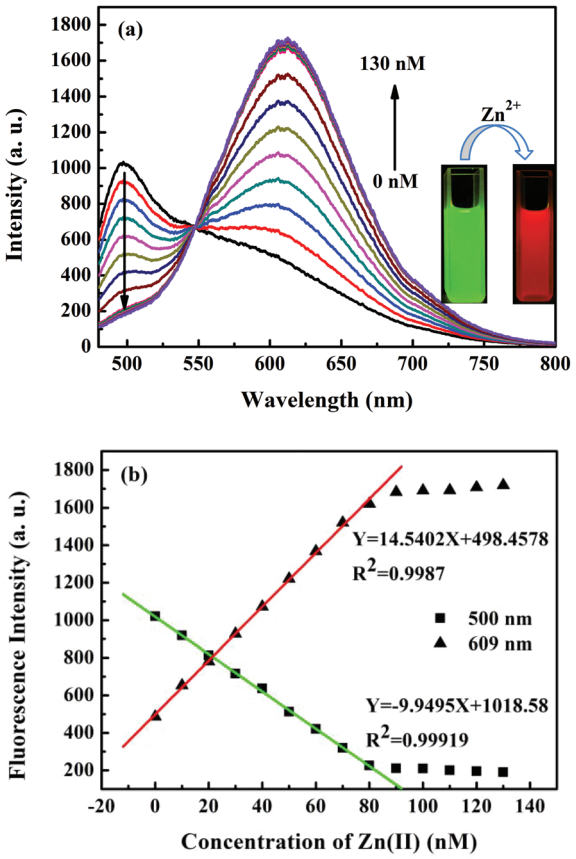

Fig. 1 (a) Fluorescence emission spectra of ZC-F4 (100 nM) excited at 468 nm upon titration of Zn^{2+} at the concentration of 0, 10, 20, 30, 40, 50, 60, 70, 80, 90, 100, 110, 120, 130 nM. Insets: luminescent photos of ZC-F4 before and after the addition of Zn^{2+} under the excitation of a 315 nm UV lamp. (b) Fluorescence intensities observed at 500 nm and 609 nm as a function of the [Zn^{2+}].

peaks located at 500 nm could be observed when excited at 468 nm. This emission band gradually disappeared with the titration of Zn^{2+} and a new emission band located at 609 nm

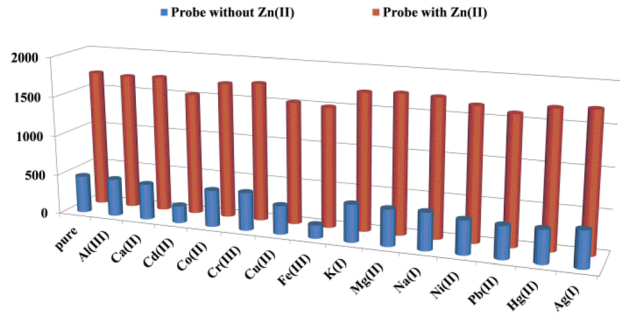

Fig. 2 Fluorescence intensities of ZC-F4 (100 nM in water–DMSO = 99 : 1) towards Zn^{2+} and various interferences (40 equiv. for K^+, Ca^{2+}, Na^+ and Al^{3+} and 20 equiv. for others) at 609 nm upon excitation at 468 nm.

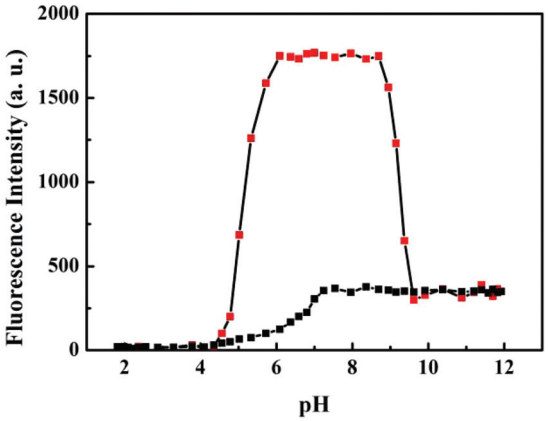

Fig. 3 Fluorescence intensities of ZC-F4 (black) and ZC-F4–Zn (red, [ZC-F4] = 100 nM, $[Zn^{2+}]$ = 100 nM) at 609 nm under various pH conditions in aqueous solution (water–DMSO = 99 : 1). λ_{ex} = 468 nm.

owing to the combination of ZC-F4 and Zn^{2+} can be observed. A significant enhancement of fluorescence intensity can be observed even when $[Zn^{2+}]$ is as low as 10 nM, which equals 0.65 ppb, indicating that ZC-F4 is highly sensitive for Zn^{2+} even at the ppb level. It is worth noting that the fluorescence intensities of ZC-F4 at both 500 nm and 609 nm have a well fitted relationship with the concentration of Zn^{2+} (Fig. 1(b)), suggesting its usage for quantitative detection of Zn^{2+}. The absorption response of ZC-F4 towards Zn^{2+} shows that the absorption maximum shifts from 450 nm to 468 nm with an isosbestic point located at 456 nm, indicating the formation of the complex of ZC-F4 with Zn^{2+} (Fig. S1†). Job's plot analysis suggests a 1 : 1 stoichiometry (Fig. S2†).

To verify the application of ZC-F4 in a complicated environment, metal ions with biological and environmental interests such as Ni^{2+}, Cd^{2+}, Cr^{3+}, Fe^{3+}, Na^+, Ca^{2+}, Pb^{2+}, Al^{3+}, Co^{2+}, Cu^{2+}, Mg^{2+}, K^+, Hg^{2+} and Ag^+ have been introduced as interferences to investigate their impact on the selectivity of ZC-F4 towards Zn^{2+}. As we can see in Fig. 2, main group metal ions and some transition metal ions, including K^+, Ca^{2+}, Na^+, Mg^{2+}, Al^{3+}, Co^{2+}, Cr^{3+}, Ni^{2+} and Pb^{2+}, have almost no influence on the fluorescence response of ZC-F4 before and after the addition of Zn^{2+}, while Cu^{2+} and Fe^{3+} exert a slight quenching effect resulting from their strong absorption of light. However, compared with the strong fluorescence enhancement caused by Zn^{2+}, their disturbances are quite minor. Although fluorescence variation could be observed when Cd^{2+} was added into ZC-F1 in our previous work, ZC-F4 shows no fluorescence response towards Cd^{2+} except a minor quenching effect. This might be due to the weaker Lewis acidity of Cd^{2+} compared with Zn^{2+}, while different molecular structures between ZC-F1 and ZC-F4 may also help to recognize Zn^{2+} from Cd^{2+}. In addition, Hg lies in the same group as Zn and Cd, but Hg^{2+} and its common disruptor Ag^+ exhibit no disturbance.

pH effect

To verify its potential usage in biology, the pH effect on the fluorescence response of the probe is investigated by plotting the fluorescence intensity of ZC-F4 with Zn^{2+} *vs.* pH values. As shown in Fig. 3, the emission intensities of the probe increased dramatically with the pH increase from 4.5 to 6 which can be ascribed to the competition between the proton and zinc ions. Meanwhile, stable fluorescence response towards Zn^{2+} can be observed in the pH range 6–9, indicating that the probe is suitable for applying in biology. The fluorescence of ZC-F4–Zn was quenched under alkaline conditions with pH > 9, which can be well explained by the formation of $Zn(OH)^-$ or $Zn(OH)_2$, thus reducing the concentration of Zn^{2+}.

Theoretical calculations

To get insight into the probing mechanism, computations on the probe before and after combination with Zn^{2+} were performed based on density functional theory (DFT).

As shown in Fig. 4, electrons are mainly localized on the coumarin part in the ground state and transfer to the carbonyl group and the atoms around when excited, indicating a moderate ICT effect in the molecule. It is worth noting that the two end-capped pyridine rings are not coplanar to the other part of the molecule, while they did not take part in electron rearrangement, suggesting its weak influence on the charge

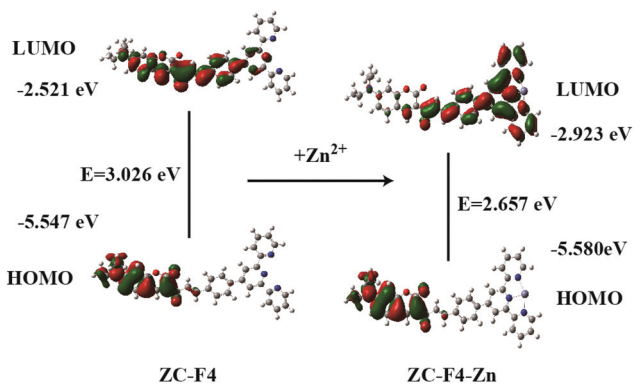

Fig. 4 HOMO–LUMO energy levels and the interfacial plots of the molecular orbitals for ZC-F4 and its complex form with Zn^{2+} (ZC-F4–Zn).

transfer effect. However, when Zn^{2+} coordinated with the probe, the electrons are still located on the coumarin part in the ground state, but are rearranged to the part from carbonyl to the terpyridine group when excited, showing that terpyridine also participates in the ICT effect. This electron rearrangement was enhanced owing to the strong electronegativity of terpyridine after combining with Zn^{2+}, resulting in a large Stokes' shift and red emission. Meanwhile, the pyridine rings have the same orientation within the conjugated plane, which may also enhance the ICT effect and fluorescence quantum yield by improving the conjugation. Thus, the enhancement of fluorescence and Stokes' shift can be seen.

Cell imaging

Since the probe has exhibited excellent sensing properties for Zn^{2+} *in vitro*, assessing whether ZC-F4 can detect Zn^{2+} in live cells is possible by labelling HeLa cells with the probe. As controls, the cells were incubated with 10 μM ZC-F4 for 30 min in DMEM medium at 37 °C, which showed strong intracellular fluorescence in the window of 480–550 nm, while no fluorescence was displayed in the detection range of 570–700 nm. Then, these cells were incubated with DMEM containing $ZnCl_2$ (5 μM) for another 15 min at 37 °C. After incubation, these cells were washed with PBS three times and a dramatically enhanced fluorescence emission in the range of 570–700 nm could be observed (excitation at 468 nm) (Fig. 5). The results of the bright-field measurements (Fig. 5a and d) suggested that the cells were viable throughout the imaging experiments upon treatment with ZC-F4 and Zn^{2+}, respectively. As depicted, these dramatic changes suggested that ZC-F4 was membrane permeable and could respond to the presence of Zn^{2+} in live cells. ZC-F4 can be supplied as a useful probe for studying the distribution and physiological activity of Zn^{2+} in live cells.

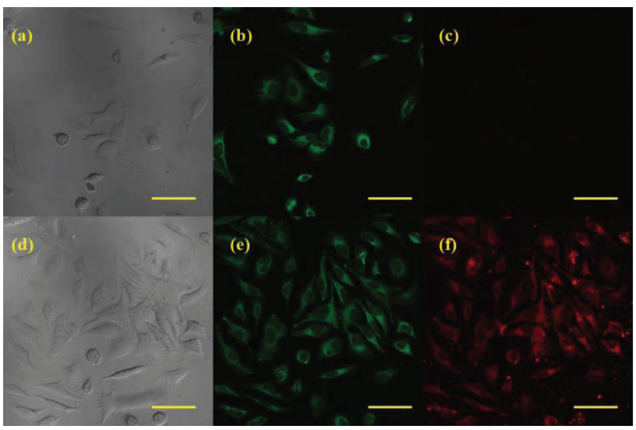

Fig. 5 Images of HeLa cells incubated with ZC-F4 (10 μM) and $ZnCl_2$ at the concentration of 0 μM (a–c) and 5 μM (d–f) for 30 min. Panels (a) and (d) show differential interference contrast (DIC) images, while panels (b), (c), (e) and (f) show the corresponding confocal fluorescence images collected at 450–530 nm (b and e) and 550–650 nm (c and f). The wavelength for excitation is 405 nm. The scale bar is 50 μm.

Conclusion

In summary, a new fluorescence probe (ZC-F4) towards Zn^{2+} was designed and synthesized and its response was studied. This probe could recognize Zn^{2+} with signals in two channels. Meanwhile, ZC-F4 was highly sensitive to Zn^{2+} at the ppb level with little disturbances from other competing metal ions, confirming its good selectivity. Furthermore, the cell imaging experiments showed that ZC-F4 was cell permeable, suitable for applying in biology, and it can be supplied as a useful probe for studying the distribution and physiological activity of Zn^{2+} in live cells.

Acknowledgements

The authors gratefully acknowledge the financial support for this work from the National Natural Science Foundation of China (no. 51010002, 51272231, 51229201 and 51372221), the Natural Science Foundation of Zhejiang Province (no. LY12E02004).

Notes and references

1 J. M. Berg and Y. Shi, *Science*, 1996, **271**, 1081–1085.
2 C. J. Frederickson and A. I. Bush, *BioMetals*, 2001, **14**, 353–366.
3 B. L. Vallee and K. H. Falchuk, *Phys. Rev.*, 1993, **73**, 79–118.
4 A. Voegelin, S. Pfister, A. C. Scheinost, M. A. Marcus and R. Kretzschmar, *Environ. Sci. Technol.*, 2005, **39**, 6616–6623.
5 X. Xie and T. G. Smart, *Nature*, 1991, **349**, 521–524.
6 S. Kury, B. Dreno, S. Bezieau, S. Giraudet, M. Kharfi, R. Kamoun and J.-P. Moisan, *Nat. Genet.*, 2002, **31**, 239–240.
7 A. I. Bush, W. H. Pettingell, M. D. Paradis and R. E. Tanzi, *J. Biol. Chem.*, 1994, **269**, 12152–12158.
8 M. P. Cuajungco and G. J. Lees, *Neurobiol. Dis.*, 1997, **4**, 137–169.
9 J.-Y. Koh, S. W. Suh, B. J. Gwag, Y. Y. He, C. Y. Hsu and D. W. Choi, *Science*, 1996, **272**, 1013–1016.
10 E. Kimura, S. Aoki, E. Kikuta and T. Koike, *Proc. Natl. Acad. Sci. U. S. A.*, 2003, **100**, 3731–3736.
11 A. Truong-Tran, J. Carter, R. Ruffin and P. Zalewski, *BioMetals*, 2001, **14**, 315–330.
12 P. D. Zalewski, I. J. Forbes, R. F. Seamark, R. Borlinghaus, W. H. Betts, S. F. Lincoln and A. D. Ward, *Chem. Biol.*, 1994, **1**, 153–161.
13 A. N. Anthemidis and C.-P. P. Karapatouchas, *Microchim. Acta*, 2008, **160**, 455–460.
14 A. C. Davis, C. P. Calloway Jr. and B. T. Jones, *Talanta*, 2007, **71**, 1144–1149.
15 G. Kaya and M. Yaman, *Talanta*, 2008, **75**, 1127–1133.
16 Z. Xu, J. Yoon and D. R. Spring, *Chem. Soc. Rev.*, 2010, **39**, 1996–2006.

17 N. Y. Baek, C. H. Heo, C. S. Lim, G. Masanta, B. R. Cho and H. M. Kim, *Chem. Commun.*, 2012, **48**, 4546–4548.
18 X. Chen, J. Shi, Y. Li, F. Wang, X. Wu, Q. Guo and L. Liu, *Org. Lett.*, 2009, **11**, 4426–4429.
19 T. Cheng, T. Wang, W. Zhu, X. Chen, Y. Yang, Y. Xu and X. Qian, *Org. Lett.*, 2011, **13**, 3656–3659.
20 H. M. Kim and B. R. Cho, *Acc. Chem. Res.*, 2009, **42**, 863–872.
21 G. Masanta, C. S. Lim, H. J. Kim, J. H. Han, H. M. Kim and B. R. Cho, *J. Am. Chem. Soc.*, 2011, **133**, 5698–5700.
22 X. Meng, S. Wang, Y. Li, M. Zhu and Q. Guo, *Chem. Commun.*, 2012, **48**, 4196–4198.
23 K. Sreenath, J. R. Allen, M. W. Davidson and L. Zhu, *Chem. Commun.*, 2011, **47**, 11730–11732.
24 H. Tian, B. Li, J. Zhu, H. Wang, Y. Li, J. Xu, J. Wang, W. Wang, Z. Sun, W. Liu, X. Huang, X. Yan, Q. Wang, X. Yao and Y. Tang, *Dalton Trans.*, 2012, **41**, 2060–2065.
25 Y. Pourghaz, P. Dongare, D. W. Thompson and Y. Zhao, *Chem. Commun.*, 2011, **47**, 11014–11016.
26 Z. Xu, K.-H. Baek, H. N. Kim, J. Cui, X. Qian, D. R. Spring, I. Shin and J. Yoon, *J. Am. Chem. Soc.*, 2009, **132**, 601–610.
27 S. Yin, J. Zhang, H. Feng, Z. Zhao, L. Xu, H. Qiu and B. Tang, *Dyes Pigm.*, 2012, **95**, 174–179.
28 L. Xue, C. Liu and H. Jiang, *Org. Lett.*, 2009, **11**, 1655–1658.
29 L. Xue, Q. Liu and H. Jiang, *Org. Lett.*, 2009, **11**, 3454–3457.
30 H. He and D. K. Ng, *Chem. –Asian J.*, 2013, **8**, 1441–1446.
31 J. Wang, W. Lin and W. Li, *Chem. –Eur. J.*, 2012, **18**, 13629–13632.
32 Y. Tan, J. Gao, J. Yu, Z. Wang, Y. Cui, Y. Yang and G. Qian, *Dalton Trans.*, 2013, **42**, 11465–11470.
33 Y. Tan, J. Yu, J. Gao, Y. Cui, Z. Wang, Y. Yang and G. Qian, *RSC Adv.*, 2013, **3**, 4872–4875.
34 Y. Tan, J. Yu, J. Gao, Y. Cui, Y. Yang and G. Qian, *Dyes Pigm.*, 2013, **99**, 966–971.
35 Y. Tan, J. Yu, Y. Cui, Y. Yang, Z. Wang, X. Hao and G. Qian, *Analyst*, 2011, **136**, 5283–5286.
36 A. Marini, A. Muñoz-Losa, A. Biancardi and B. Mennucci, *J. Phys. Chem. B*, 2010, **114**, 17128–17135.
37 R. S. Mulliken, *J. Phys. Chem.*, 1952, **56**, 801–822.
38 R. S. Mulliken, *J. Am. Chem. Soc.*, 1952, **74**, 811–824.
39 J. Wu, W. Liu, J. Ge, H. Zhang and P. Wang, *Chem. Soc. Rev.*, 2011, **40**, 3483–3495.
40 Z. Jiang, H. Lv, J. Zhu and B. Zhao, *Synth. Met.*, 2012, **162**, 2112–2116.
41 A. D. Becke, *J. Chem. Phys.*, 1993, **98**, 5648.
42 W. J. Hehre, *J. Chem. Phys.*, 1972, **56**, 2257.
43 M. Cossi, N. Rega, G. Scalmani and V. Barone, *J. Comput. Chem.*, 2003, **24**, 669–681.
44 J. Tomasi, B. Mennucci and R. Cammi, *Chem. Rev.*, 2005, **105**, 2999–3094.
45 M. J. Frisch, G. W. Trucks, H. B. Schlegel, G. E. Scuseria, M. A. Robb, J. R. Cheeseman, G. Scalmani, V. Barone, B. Mennucci, G. A. Petersson, H. Nakatsuji, M. Caricato, X. Li, H. P. Hratchian, A. F. Izmaylov, J. Bloino, G. Zheng, J. L. Sonnenberg, M. Hada, M. Ehara, K. Toyota, R. Fukuda, J. Hasegawa, M. Ishida, T. Nakajima, Y. Honda, O. Kitao, H. Nakai, T. Vreven, J. A. Montgomery Jr., J. E. Peralta, F. Ogliaro, M. Bearpark, J. J. Heyd, E. Brothers, K. N. Kudin, V. N. Staroverov, R. Kobayashi, J. Normand, K. Raghavachari, A. Rendell, J. C. Burant, S. S. Iyengar, J. Tomasi, M. Cossi, N. Rega, J. M. Millam, M. Klene, J. E. Knox, J. B. Cross, V. Bakken, C. Adamo, J. Jaramillo, R. Gomperts, R. E. Stratmann, O. Yazyev, A. J. Austin, R. Cammi, C. Pomelli, J. W. Ochterski, R. L. Martin, K. Morokuma, V. G. Zakrzewski, G. A. Voth, P. Salvador, J. J. Dannenberg, S. Dapprich, A. D. Daniels, Ö. Farkas, J. B. Foresman, J. V. Ortiz, J. Cioslowski and D. J. Fox, *R. A. Gaussian 09*, Gaussian, Inc., Wallingford CT, 2009.
46 J. Delcamp, Y. Shi, J. Yum, T. Sajoto, E. Dell'orto, S. Barlow, M. Nazeeruddin, S. Marder and M. Gratzel, *Chem. –Eur. J.*, 2013, **19**, 1819–1827.
47 N. Karton-Lifshin, L. Albertazzi, M. Bendikov, P. S. Baran and D. Shabat, *J. Am. Chem. Soc.*, 2012, **134**, 20412–20420.
48 Y.-Y. Wu, Y. Chen, G.-Z. Gou, W.-H. Mu, X.-J. Lv, M.-L. Du and W.-F. Fu, *Org. Lett.*, 2012, **14**, 5226–5229.
49 Y. Tan, Q. Zhang, J. Yu, X. Zhao, Y. Tian, Y. Cui, X. Hao, Y. Yang and G. Qian, *Dyes Pigm.*, 2013, **97**, 58–64.
50 H. M. Kim, M. S. Seo, M. J. An, J. H. Hong, Y. S. Tian, J. H. Choi, O. Kwon, K. J. Lee and B. R. Cho, *Angew. Chem., Int. Ed.*, 2008, **47**, 5167–5170.
51 D. M. Nguyen, A. Frazer, L. Rodriguez and K. D. Belfield, *Chem. Mater.*, 2010, **22**, 3472–3481.
52 B. Zhu, C. Gao, Y. Zhao, C. Liu, Y. Li, Q. Wei, Z. Ma, B. Du and X. Zhang, *Chem. Commun.*, 2011, **47**, 8656–8658.